Ground-Based Measurements of Ozone and NO_2 during MANTRA 1998 Using a Zenith-Sky Spectrometer

Matthew R. Bassford[1†], Kimberly Strong[1*], Chris A. McLinden[2] and C. Thomas McElroy[2]

[1]*Department of Physics, University of Toronto*
60 St. George St.
Toronto ON M5S 1A7
[2]*Air Quality Research Branch, Meteorological Service of Canada*
Downsview ON

[Original manuscript received 22 August 2000; in revised form 9 August 2002]

ABSTRACT *A portable ground-based instrument has been constructed for the automated measurement of vertical column abundances of a number of gases pertinent to stratospheric ozone chemistry. The instrumentation is described in this paper and results are presented from the first set of field measurements, made during the Middle Atmosphere Nitrogen TRend Assessment (MANTRA) 1998 field campaign at Vanscoy, Saskatchewan, Canada. Zenith-sky spectra in the near ultraviolet and visible wavelength regions were recorded for a period of seven days, prior to and following the launch of the MANTRA balloon on 24 August 1998. The spectra were then analysed using the differential optical absorption spectroscopy (DOAS) technique in conjunction with a radiative transfer model to determine vertical column amounts of ozone and NO_2. Ozone measurements compared favourably with concurrent observations by ozonesondes, a Brewer spectrophotometer, and satellite instruments. Vertical NO_2 columns were in broad agreement with those determined by the Global Ozone Monitoring Experiment (GOME) satellite instrument.*

RÉSUMÉ *[Traduit par la rédaction] Un instrument terrestre portable a été construit pour mesurer automatiquement l'abondance, dans une colonne verticale, de divers gaz ayant un rôle à jouer dans la chimie de l'ozone stratosphérique. Cet article décrit l'instrumentation et présente les résultats du premier ensemble de mesures faites dans le cadre de l'étude sur le terrain de 1998 pour l'Évaluation des tendances de l'azote dans l'atmosphère moyenne (MANTRA), à Vanscoy, en Saskatchewan, au Canada. Des spectres du ciel au zénith dans les régions de longueurs d'ondes visible et proche-ultraviolet ont été enregistrés sur une période de sept jours, avant et après le lancement du ballon MANTRA le 24 août 1998. Les spectres ont ensuite été analysés au moyen de la technique spectroscopique d'absorption optique différentielle (DOAS) de pair avec un modèle de transfert radiatif pour déterminer les quantités d'ozone et de NO_2 dans une colonne verticale. Les mesures d'ozone ont bien soutenu la comparaison avec les observations par sondes d'ozone, par spectrophotomètre Brewer et par satellite faites au même moment. Les colonnes verticales de NO_2 s'accordaient généralement avec celles mesurées par l'instrument du satellite de l'Expérience de surveillance mondiale de l'ozone (GOME).*

1 Introduction

The discovery of the Antarctic ozone hole (Farman et al., 1985) prompted a re-examination of the science governing ozone concentrations in the middle atmosphere. To date, the major mechanistic pathways for stratospheric ozone depletion have been established and models simulating ozone processes at mid-latitudes are broadly consistent with observed mid-latitude trends (WMO, 1999). However, unravelling an overall negative trend in mid-latitude ozone columns from natural variability in stratospheric composition presents a more complicated challenge. Natural fluctuations in ozone columns occur due to atmospheric dynamics and seasonal changes; in addition, volcanic activity and the 11-year solar cycle modify ozone chemistry. These effects occur on quite different timescales and can mask any anthropogenic influence. Furthermore, it is still unclear what proportion of mid-latitude ozone loss is due to transport of ozone-depleted air from polar regions, and what proportion is due to chemical depletion at mid-latitudes (Hadjinicolaou et al., 1997). This uncertainty is particularly large for ozone loss in the lower stratosphere (15–20 km). In contrast with mid-latitude trends, Arctic ozone loss during the 1990s was pronounced (Fioletov et al., 1997). Very low ozone column amounts were observed in six of the late-winter/spring periods, during years with a

†Current affiliation: Ministry of Defense, Bristol, United Kingdom
*Corresponding author's e-mail: strong@atmosp.physics.utoronto.ca

cold and persistent winter Arctic vortex. In fact, future Arctic ozone depletion will likely be enhanced by a colder stratosphere (induced by increasing CO_2 concentrations) coupled with near present-day chlorine loading. Modelling studies (Austin and Butchart, 1994; Shindell et al., 1998) suggest that the Arctic stratosphere will be primed for severe ozone losses for the next 10–20 years.

Stratospheric observations from ground-based, balloon-borne and satellite instruments are complementary. Ground-based instruments can be utilized for long-term measurements at a particular site and also have the flexibility of being transportable to different locations. Measurements from a suite of balloon-borne instruments can characterize stratospheric composition at a specific time and place. Satellite observations provide a long-term global picture. It is important to collect and collate high-quality measurements of stratospheric ozone and the trace species that influence ozone concentrations at regular locations around the globe. The rationale behind this mandate is threefold:

1. to monitor stratospheric ozone and other trace gases as anthropogenic emissions evolve;
2. to test and refine stratospheric models, for example in Langrangian-type experiments where an air mass is monitored over time while subjected to chemistry and transport; and
3. to provide more information as to the relative magnitude of natural variability in ozone levels compared with change stimulated by anthropogenic activity.

The detection of stratospheric constituents from the ground by measuring the absorption of sunlight scattered from the zenith sky is well established; it was first applied to ozone (Dobson and Harrison, 1926; Dobson, 1957) and NO_2 (Brewer et al., 1973) using measurements of intensity at a few discrete wavelengths. This method was improved by Noxon (Noxon, 1975; Noxon et al., 1979), who recorded spectra in the range of 435 to 450 nm, then ratioed twilight spectra to a noon reference in order to remove solar Fraunhofer lines, and used the differential change in absorption to measure the column abundance of NO_2. Syed and Harrison (1980) made similar measurements and compared the results of using the absorption at a number of discrete wavelengths with the use of a continuous spectrum to derive NO_2 vertical column abundances. Platt et al. (1979) developed a variation of this technique to measure the absorption in long horizontal tropospheric paths using an artificial light source. In addition to ozone and NO_2, differential optical absorption spectroscopy (DOAS) has been used successfully to measure vertical columns of OClO (Solomon et al., 1987a), BrO (Solomon et al., 1989), and NO_3 at night using direct viewing of the moon (Noxon et al., 1978). Efforts have also been made to obtain vertical profiles of NO_2 from the change in retrieved DOAS slant column with solar zenith angle during twilight (McKenzie et al., 1991; Preston et al., 1997, 1998).

Ultraviolet (UV)–visible spectroscopy continues to play an important role in monitoring the stratosphere, having been selected as one of the primary measurement techniques in the Network for the Detection of Stratospheric Change (NDSC). A number of groups have developed their own UV–visible zenith-sky instrumentation (e.g., Eisinger et al., 1997; Fish et al., 1995; Gil et al., 2000; Koike et al., 1999; Liley et al., 2000; Otten et al., 1998; Roscoe et al., 1997; Van Roozendael et al., 1994). The SAOZ (Systeme d'Analyse et d'Observations Zenithales) is of particular note, as a network of these spectrometers are now deployed worldwide (Pommereau and Goutail, 1988; Goutail et al., 1994; Sarkissian et al., 1997).

The NDSC coordinates a long-term program of stratospheric measurements using a number of validated UV–visible spectrometers. Details of the instruments that form the observational network are given on the NDSC website (http://www.ndsc.ncep.noaa.gov). A recent intercomparison of NDSC instruments using observations of ozone and NO_2 is presented by Roscoe et al. (1999). Earlier intercomparisons of UV–visible spectrometers, including most of the instruments referenced above, are described by Hoffman et al. (1995) and Vaughan et al. (1997).

In order to extend the geographic coverage of the current observational network and increase the number of instruments for the cross-comparison and validation of measurements, we have constructed a ground-based spectrometer (GBS). The instrument observes zenith-scattered sunlight at UV–visible wavelengths and was developed in order to make automated measurements of stratospheric ozone, NO_2, BrO and OClO. The spectrometer is furnished with an adjustable entrance slit, a triple-diffraction-grating turret, and a charge-coupled device (CCD) array detector; this combination provides a wide spectral range, with good spectral resolution and sampling efficiency. The robust nature of the instrument described here means that it is ideally suited to measurements in remote locations; it is contained in a weatherproof, thermostatically controlled box and operates in a stand-alone manner with little maintenance required. It was deployed for the first time during the Middle Atmosphere Nitrogen TRend Assessment (MANTRA) 1998 field campaign (Strong et al., this issue) to complement the other ground-based and balloon-borne measurements.

2 Experimental methodology

a *Instrumentation*

The instrumentation consisted of three main components (Fig. 1) housed in a watertight aluminum box (0.8 m × 0.8 m × 0.5 m) with a top-mounted plexiglas window (UV-grade) to provide a zenith view of the sky. In brief, zenith-scattered sunlight was focused onto the entrance slit of an imaging spectrometer that dispersed the light onto a CCD array detector. The aluminum box was portable, yet durable enough to be operated outdoors in the field environment. A heating circuit and a temperature monitor were installed inside the box to provide control of the internal temperature.

Initially, the entrance optics were comprised of a mirror with enhanced UV reflectivity (100 mm × 100 mm, aluminum

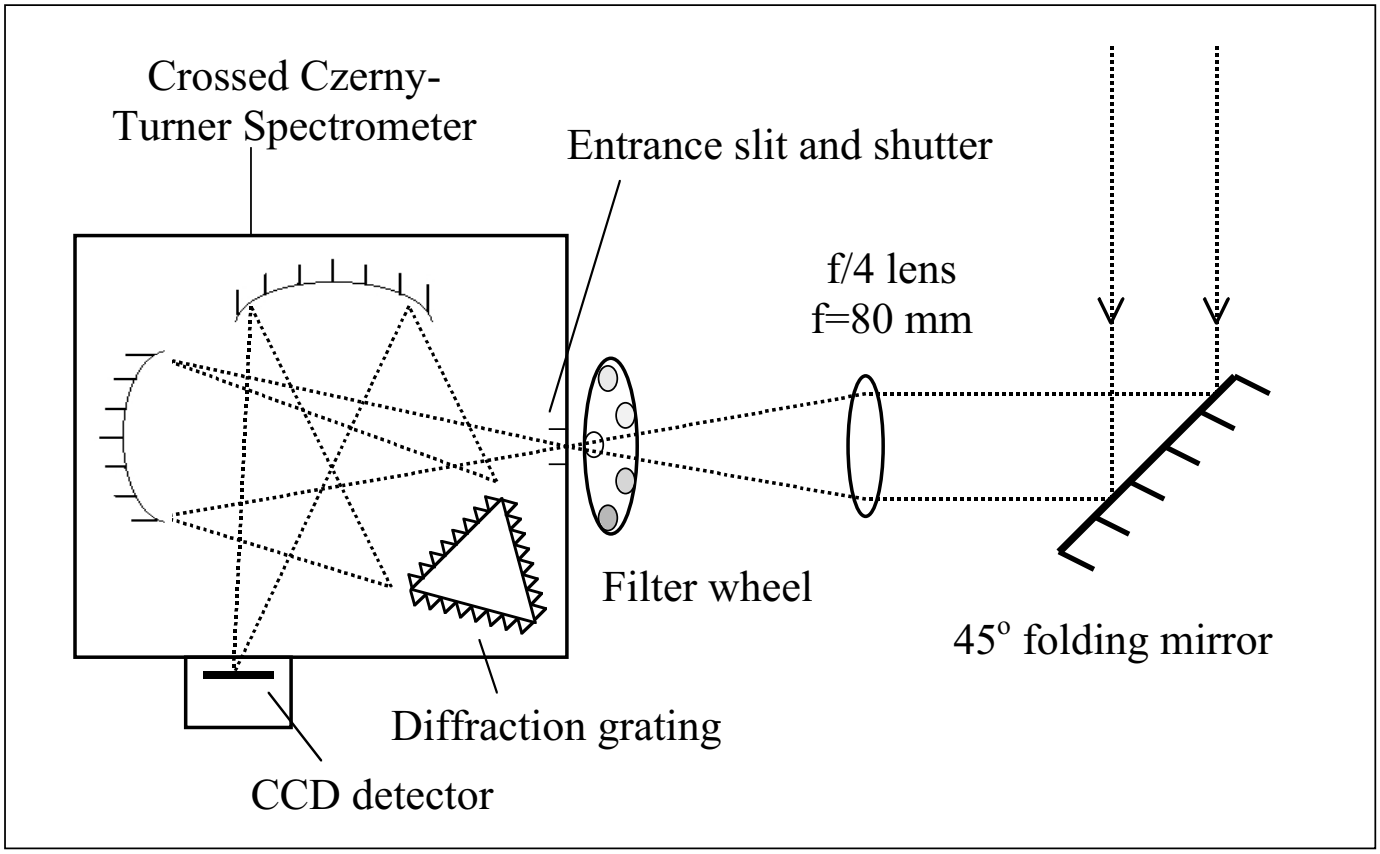

Fig. 1 Optical layout of the zenith-sky grating spectrometer.

TABLE 1. Spectral resolution and range of the grating spectrometer

Grating (grooves mm^{-1})	Spectral Bandwidth (nm)	Nominal Wavelength Range (nm)	Entrance Slit Width (μm)	FWHM[a] (nm)
400	360	320–680	50	2.0
			100	2.2
			200	2.9
600	234	320–554	50	0.9
			100	1.2
			200	1.8
1800	66	320–386	50	0.5
			100	0.6
			200	0.7

[a]Instrument resolution was determined by measuring the full width at half maximum (FWHM) of two mercury emission lines (436 and 546 nm) centred on the CCD array.

coated, Melles Griot Inc., Irvine, CA, USA) mounted at 45° to fold sunlight scattered from the zenith into the horizontal plane. Incoming light was focused onto the entrance slit of the spectrometer by means of a fused silica lens (diameter = 22.4 mm, f/4, Melles Griot). All entrance optics were well baffled to reduce stray light, and a filter (350–600 nm, filter # BG-38, Andover Corp., Salem, NH, USA) was mounted between the lens and the spectrometer to eliminate light outside the spectral range of interest. Since the MANTRA 1998 campaign, this simple arrangement has been modified to include a liquid light guide (core diameter = 3 mm, length = 1 m, Oriel Instruments, Stratford, CT, USA) to depolarize incoming sunlight prior to dispersion. In the revised configuration, zenith-scattered light is focused through a fused silica lens (diameter = 40 mm, f/2.5) mounted inside a cylindrical baffle, and is conducted through the liquid light guide (LLG). The divergent light emerging from the LLG enters a cylindrical baffled f/# matcher where it is collimated and then re-focused onto the entrance slit of the spectrometer. With this arrangement, about 60% of the 12-mm height of the slit is usefully illuminated.

The imaging spectrometer (Triax 180, Instruments S. A. Inc., Edison, NJ, USA) utilized a crossed Czerny-Turner

geometry with aspherical optics to correct astigmatism, generate a flat-field output, and provide point-to-point imaging. It had a focal length of 0.190 m (f/3.9) and a 12 mm × 30 mm focal plane. It was fitted with an adjustable entrance slit and a triple-grating turret, which results in some degree of flexibility in terms of resolution and spectral range. The turret was mounted with diffraction gratings of 400, 600 and 1800 grooves mm^{-1} at blaze wavelengths of 550, 400 and 500 nm, respectively. Table 1 summarizes the resolution characteristics of each grating determined by measuring two mercury emission lines (436 nm and 546 nm). During the MANTRA campaign, spectra were acquired with a slit width of 50 μm and the 600-grooves mm^{-1} diffraction grating. The resulting spectral resolution (0.9 nm as defined by the full width at half maximum (FWHM) of the lines) was sufficient to retrieve accurate NO_2 columns (Roscoe et al., 1996). The FWHM was determined using Spectramax software (Instruments S. A.) to fit a Gaussian function to the pixel column values. During a separate measurement campaign in the Arctic, the 1800-grooves mm^{-1} diffraction grating was used on occasion, in order to improve the spectral resolution and the signal-to-noise ratio in the BrO/OClO region of the spectrum. Routine daily measurements were acquired using the 600-grooves mm^{-1} grating.

A CCD array detector was employed (Instruments S. A. "Spectrum One" with a SITe chip of 800 × 2000 pixels, each 15 μm × 15 μm), which provided an active area of 12 mm × 30 mm to match the focal plane of the spectrometer. The sampling ratio of the detector (8.5 pixels nm^{-1} for the 600 grooves mm^{-1} grating used in this work, 5.5 and 30 pixels nm^{-1} for the 400 and 1800 grooves mm^{-1} gratings, respectively) was high enough to minimize interpolation errors that can arise due to under-sampling (Roscoe et al., 1996). The CCD was operated in multi-pin phased mode and thermoelectrically cooled to –30°C to reduce dark current, and was back-illuminated with an anti-reflection coating to improve quantum efficiency of the detector in the UV region. On-chip binning of each pixel column (each column consisting of 800 pixels) was performed to maximize the signal-to-noise ratio.

The CCD was characterized in the laboratory before and after the field measurements, and preprocessing of the raw spectra included the removal of detector bias (a small, constant electronic offset present in the signal) and dark current for each of the 2000 pixel columns. Due to small differences in the dark current and bias characteristics of each pixel column, preprocessing was performed for each column individually. Such differences arise due to slight inconsistencies in pixel size or coating thickness. Dark current measurements were made by sheathing the instrumentation in black cloth and recording spectra for a range of integration times. The dark current of each pixel column of the detector increased linearly with integration time, which means that bias could be experimentally derived by extrapolating the dark current to zero integration time. Artefacts caused by signal-dependent dark current that have been observed in detectors that use linear diode arrays of p-n junctions (Stutz and Platt, 1992) were insignificant or absent in our CCD array, which is a Metal Oxide Semiconductor (MOS) device. A further advantage of CCD arrays over linear diode arrays is the absence of Fabry-Pérot etalon structure inherent in many diode array detectors (Mount et al., 1992). Dark current measurements were also made during the field campaign.

During the MANTRA campaign, it was determined that the dark current was of the order of 150 counts s^{-1} for each column of 800 pixels. This corresponds to a dark current signal of less than three counts for a reference spectrum taken at a solar zenith angle (SZA) of 40° (exposure time ≈ 0.02 s). For twilight spectra acquired at SZAs of 90° and 95° (corresponding to exposure times ≈ 0.5 s and ≈ 15 s) the dark current was typically 75 counts and 2250 counts respectively. The typical bias for a pixel column was determined to be about 800 counts. Compared with the total signal of the raw spectra (prior to subtraction of dark current and bias) of approximately 60,000 counts, the dark current contribution was 0.125% at SZA = 90°, and 3.75% at SZA = 95°.

A characterization of inter-pixel variability (which arises due to small differences in the sensitivity of pixels to light) was also attempted by removing the diffraction grating and illuminating the CCD (thereby removing wavelength dependence). However, applying a correction for inter-pixel variability to the spectra was found to have little effect (in some cases a slightly detrimental effect) on the quality of the differential spectra. The correction factors were very small and it is believed that any inter-pixel variability was effectively 'averaged out' through the binning of 800 individual pixels. The detrimental effect on some spectra can be assigned to experimental error in determining inter-pixel variability; a more extensive characterization study would confirm this.

In summary, in its current configuration, this new instrument offers the following advantages: (1) depolarizing input optics (not installed for this work); (2) a versatile spectrometer (adjustable entrance slit and triple-grating turret) that enables a choice of resolution and spectral range; (3) a cooled CCD array detector, free of etalon effects and having 2000 pixels along the 30-mm-long wavelength axis to provide an excellent sampling ratio; (4) a portable, weatherproof, temperature-stabilized box; and (5) stand-alone automated operation with customized data acquisition software that can be remotely accessed (see following, implemented after this work).

b *Field Measurements*

The instrument was deployed as part of the MANTRA 1998 field campaign at Vanscoy, SK (52° 01′N, 107° 02′W, elevation 511 m). Vertical column measurements were retrieved from the twilight zenith-sky spectra recorded during 18–25 August (Julian day 230–237). An overview of the MANTRA field campaign is presented elsewhere (Strong et al., this issue).

c *Operating Procedure*

Twilight zenith-sky spectra (320–554 nm) were recorded daily at solar zenith angles from 80° to 96° during both sunrise

and sunset. In addition, a set of daily reference spectra was acquired around local noon when the SZA was between 40° and 50°. The signal-to-noise ratio of each spectrum was increased by averaging 20–255 repeated scans. Exposure time was varied with changing light levels to maximize the total signal, and the number of accumulations comprising a spectral set was simultaneously varied to restrict the total accumulation time to five minutes. At a mid-latitude site such as Vanscoy, a five-minute interval corresponds to a change in solar zenith angle of 0.7° (when SZA = 90°).

The spectrometer can be controlled either by means of a laptop computer contained within the aluminum box (networked using an Ethernet cable running indoors) or using a desktop computer and a General Purpose Interface Bus (GPIB) extension cable (National Instruments, Austin, TX, USA). During the MANTRA campaign, the system was operated using the desktop configuration for logistical reasons. However, both configurations have been used successfully. In order to correct for drift in the computer clock, an automatic adjustment was made every 12 hours to align the clock with a networked timeserver (at internet address clock.psu.edu). During the MANTRA campaign, proprietary software (Spectramax, Instruments S. A.) was used to control spectrometer settings and data acquisition; however, customized LabVIEW software has since been written to facilitate unattended long-term measurements. One refinement is an adaptive routine that optimizes integration time depending on light intensity. The system is now truly stand-alone and unattended collection of zenith-sky spectra is possible. Further automation of the measurements has been achieved by the use of remote-access software (pcANYWHERE, Symantec Corp, Cupertino, CA, USA) that allows spectrometer control from a remote site.

Unfortunately, the instrument spectral range was compromised during the MANTRA campaign because a portion of the CCD array developed an electronic defect, thought to be associated with the collection of signal following on-chip binning. Data from approximately 535 of the 2000 pixel columns were corrupted. For spectral observations in the wavelength range of 320 to 554 nm, this corresponded to the region between 330 and 390 nm. This unfortunate artefact precluded the possibility of concurrent observations of BrO alongside ozone and NO_2. However, ozone and NO_2 measurements were unaffected because the absorption features used to determine column abundances were at longer wavelengths: 470–540 nm (ozone) and 405–450 nm (NO_2). The CCD array has since been successfully repaired.

3 Retrieval methodology

a *The Retrieval of Vertical Column Information*

Spectra were analysed using the DOAS technique, a relatively simple and well-established method for determining the amount of trace gas along a path. Zenith-sky DOAS has been widely employed to measure vertical column densities of stratospheric gases such as ozone, NO_2, BrO and OClO, as discussed in Section 1. Comprehensive explanations of DOAS theory have been presented elsewhere (Solomon et al., 1987b; Platt, 1994; Platt et al., 1997). In essence, the zenith-sky DOAS technique utilizes the fact that scattered sunlight observed at twilight traverses a much longer stratospheric path than scattered sunlight observed at noon. For species with the bulk of absorbing molecules in the stratosphere, the apparent slant column density (*SCD*; the number density integrated along the photon path) is therefore much greater in twilight spectra.

For twilight spectra recorded during the MANTRA campaign, a noon spectrum measured on Julian day (J-day) 237 (25 August) 1998 was used as a common Fraunhofer reference spectrum. Most recent publications that present ozone and NO_2 measurements also use a common reference, rather than a daily reference spectrum (e.g., Roscoe et al., 1999). The benefits of using a single reference are twofold. Differential slant columns of ozone and NO_2 from different days can be directly compared as each value is relative to the same spectrum; any systematic errors in the reference spectrum are therefore constant and do not affect trends. Secondly, a reference spectrum from a cloudless day can be selected in order to reduce the influence of tropospheric absorbers.

The optical depth for each twilight measurement as a function of wavelength, $OD(\lambda)$, was calculated from Eq. (1) (see Perrin, 1948), where I and I_o correspond to the intensity of the twilight and reference spectra respectively:

$$OD(\lambda) = -\ln \frac{I(\lambda)}{I_o(\lambda)}. \quad (1)$$

A third-order polynomial was subtracted from the optical depth to approximate aerosol scattering. Next, differential cross-sections of absorbing gases (derived by subtracting a second-order polynomial from laboratory cross-sections) were simultaneously fitted to the differential spectrum using a non-linear (Marquart-Levenberg) least-squares fitting routine (Press et al., 1992). The Ring effect was treated as a quasi-linear absorber in cross-section space using a modelled Ring cross-section calculated by Chance and Spurr (1997). An iterative shifting and stretching algorithm was used to correct small changes in wavelength calibration and spectral dispersion of the spectrometer. Cross-sections fitted to the differential spectra were as follows: ozone and NO_2 at 221 K (Burrows et al., 1999a, 1998, respectively), H_2O (Sarkissian, 1992) and O_4 (Greenblatt et al., 1990). Each highly sampled cross-section was smoothed with a Gaussian function, which provided a reasonable approximation to the measured slit function.

Typical differential spectra for ozone and NO_2 are presented in Fig. 2, alongside fitted spectra. Residual structure is also plotted, that is the difference between the observed and the fitted spectra. The root-mean-square (r.m.s.) residuals for the ozone and NO_2 fits shown were 2.02×10^{-3} and 2.09×10^{-3} respectively. While the fitted spectra are considered adequate for accurately retrieving total column amounts of ozone and NO_2, the residuals are larger than those obtained from certain

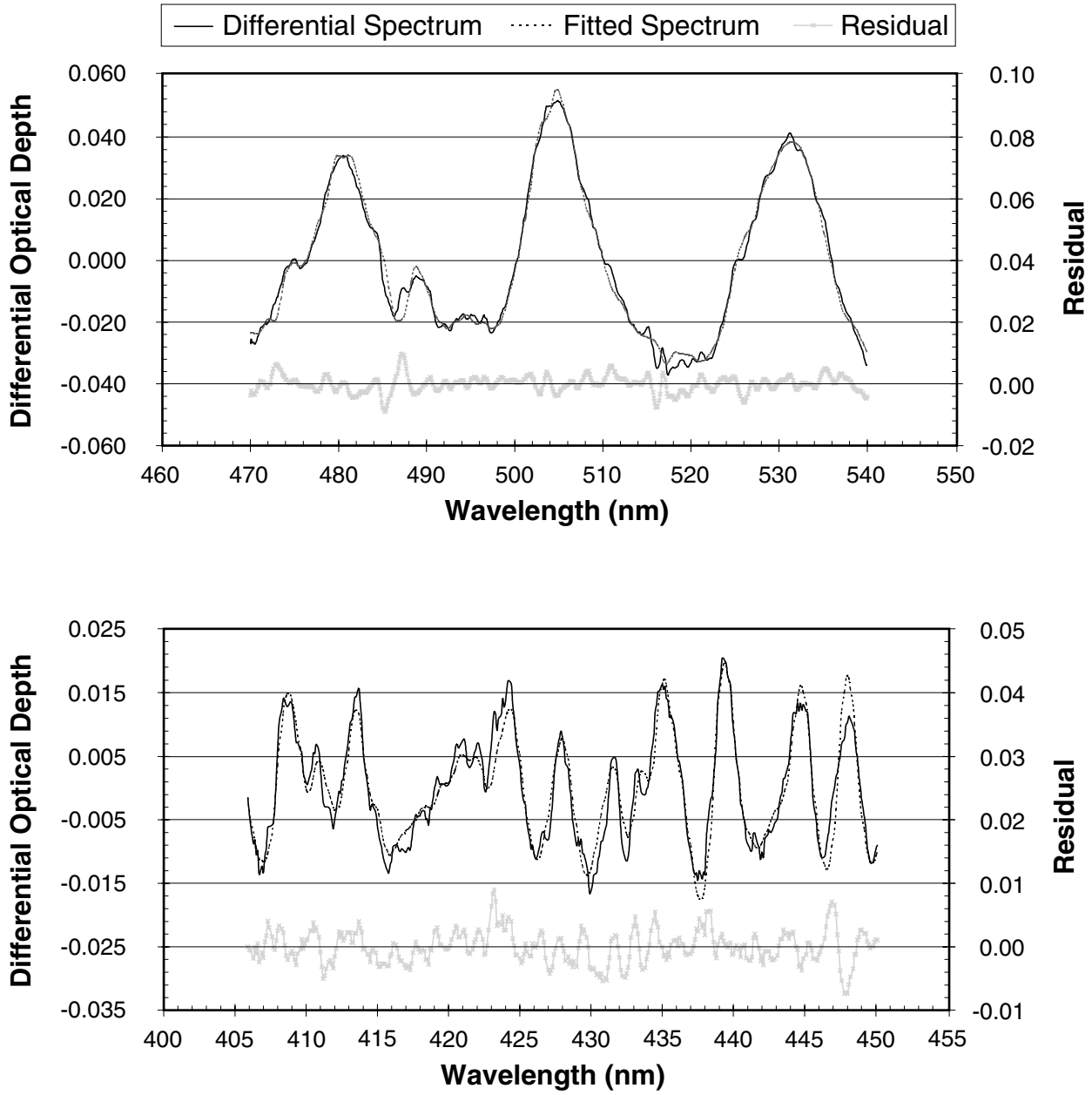

Fig. 2 Differential and fitted spectra in the wavelength regions of the Chappuis ozone (upper plot) and the NO_2 (lower plot) absorption bands. The residual is also plotted and is the difference between the observed and the fitted spectra.

state-of-the-art instruments that participated in the recent NDSC intercomparison exercise (Roscoe et al., 1999). The residuals obtained from our instrument during the MANTRA campaign exhibit systematic, or pseudo-random features. We believe that these arise from a number of sources, namely: polarization artefacts, features generated by corrupted pixels on the CCD, and an insufficient correction for the Ring Effect. All three of these problems have since been addressed: by introducing a polarization-scrambling LLG into the optical path, by repairing the CCD anomaly, and by investigating the use of an alternative method of correcting for the Ring Effect (Sioris and Evans, 1999).

From the fitted optical depth of each absorber, the differential *SCD* was retrieved. The apparent vertical column density at SZA θ, $VCD(\theta)$, is related to the fitted *SCD*, $SCD(\theta)$, as shown in Eq. (2):

$$VCD(\theta) = \frac{SCD(\theta) + RCD}{AMF(\theta)} \tag{2}$$

where the reference column density (*RCD)* is the slant column density of absorber present in the reference spectrum, derived by constructing Langley plots as described in Section 4a.

TABLE 2 Summary of measurement errors

Error	Ozone	NO_2	Source
Random noise	1%	2%	Statistically calculated from measurements
Instrument error (dark current, bias, slit function)	3%	3%	Informed estimate
Pseudo-random errors	1–2%	4–6%	Derived from measurements
Absolute cross-sections	2.6%	2.3%	Burrows et al., (1999a, 1998) respectively
Temperature dependence of the NO_2 cross-section	–	< 8%	Pfeilsticker et al., 1999b
Uncertainty in NO_2 *RCD*	–	1–3%	Derived from measurements
AMF error	2%	5%	Calculated for our RT model
Filling in of absorption by Raman scattering	1%	5%	Fish and Jones (1995); Pfeilsticker et al., (1999b)
Total r.m.s. error	±5%	±12–13%	

$AMF(\theta)$ is the air mass factor, calculated using a radiative transfer (RT) model (McLinden et al., 2002) that models the path of zenith-scattered light using successive orders of scattering in an inhomogeneous atmosphere. The RT model atmosphere was parametrized as follows. Vertical profiles for air number density, temperature and ozone were generated by averaging data from three sonde flights (11, 18 and 23 August 1998) mapped onto a 0.5-km vertical grid (J. Davies, personal communication, 1999). A Gaussian NO_2 profile having a maximum of 10.7 ppbv at 34 km and a FWHM of 14 km was used, along with a stratospheric sulphate profile derived from summer mid-latitude (August 1997, 50°N) Stratospheric Aerosol and Gas Experiment (SAGE) II extinction coefficient measurements (Thomason et al., 1997). The Earth's surface was considered to be Lambertian with an albedo of 0.2. Ozone and NO_2 absorption cross-sections (Burrows et al., 1999a, 1998) were varied with altitude to account for temperature changes.

It should be noted that on overcast days, cloud layers representative of the observed meteorological situation (T. Mathews, personal communication, 1999) were inserted into the RT model and revised *AMF*s calculated. Clouds were classified into three rudimentary types: high altitude cirrus (9 km, optical depth = 0.1), altocumulus (3–5 km, optical depth = 10) or low-level cumulus cloud (1–3 km, optical depth = 100). In common with other reports (e.g., Erle et al., 1995, Pfeilsticker et al., 1999a) clouds were found to exert a strong influence on the slant column amounts retrieved. It should be noted that a quantitative understanding of absorption and scattering of photons within tropospheric clouds presents a formidable challenge. There remains some debate regarding the mechanism by which clouds influence zenith-sky spectra and enhance the apparent optical depths of ozone and NO_2. We have performed a thorough study on the effect of clouds on our zenith-sky measurements (Bassford et al., 2001), in which this topic and likely mechanisms are discussed in more detail. A thunderstorm on the evening of 22 August prevented the retrieval of accurate columns of ozone and NO_2 and no data for this period are shown here.

b *An Estimate of Measurement Error*

The total measurement error for the ozone and NO_2 observations was estimated from the root-sum-square of individual errors. These errors are summarized in Table 2. Firstly, the random noise on the spectra was statistically calculated (using the method described by Sarkissian (1992) and found to be 1% for ozone and 2% for NO_2. Measurements of dark current and bias were recorded throughout the measurement campaign and exhibited variability and a tendency to drift over time. Combined with the fact that the measured instrument slit function was not strictly Gaussian (as assumed in smoothing the fitted cross-sections), instrument errors were estimated to contribute 3% to the total error. Pseudo-random errors (which result in unaccounted-for structure in the DOAS spectra) were typically 1–2% for ozone and 4–6% for NO_2.

Uncertainties in the ozone and NO_2 cross-sections are 2.6% and 2.3%, respectively (Burrows et al., 1999a, 1998). The strong temperature dependence of the NO_2 cross-section was accounted for in the calculation of *AMF*s but a single NO_2 cross-section at 221 K was used in the DOAS fitting. This is a reasonable value for a stratospheric absorber (e.g., Vandaele et al., 1998), but uncertainty in the temperature at which most of the NO_2 is located can generate a systematic error of as much as 8% for an instrument of comparable resolution to ours (Pfeilsticker et al., 1999b). When the value of the NO_2 *RCD* was varied by $\pm 2 \times 10^{15}$ molecules cm^{-2}, an error of 1–3% was introduced in the retrieved NO_2 *VCD*. Finally, an error was derived for the calculated *AMF*s due to approximations in the RT model. Following a study we conducted into parametrization of the RT model (Bassford et al., 2001) it was concluded that the error arising from uncertainties in the *AMF* calculation was probably less than 2% for ozone but approximately 5% for NO_2 (largely due to uncertainty in the shape of the NO_2 profile used).

The retrieved NO_2 slant columns have not been corrected for the 'filling-in' of NO_2 absorption features by multiple Raman scattering. This effect can result in an underestimation of the NO_2 columns by 8% (at sunset) to 10% (at sunrise) at 90° for a polarization-sensitive spectrometer (Fish and Jones, 1995). Pfeilsticker et al. (1999b) have shown that convolution with an instrument function of similar resolution to ours reduces this effect to about 5%. This effect is small (approximately 1%) for ozone.

The total error (root-sum-square) was determined to be ±5% for ozone and ±12–13% for NO_2. The smallest errors occurred around 90° where there was a large difference in *AMF*s between the twilight and the reference spectra yet sufficient light intensity to collect spectra in a reasonably short (0.5 s) integration time.

4 Results

a *Ozone Measurements*

Vertical ozone columns for each set of twilight observations were calculated from Langley plots, whereby apparent ozone slant columns at different SZAs were plotted against their corresponding *AMF*s. A typical Langley plot for sunrise on 20 August 1998 (J-day 232) is shown in Fig. 3. The slope of the line is equal to the vertical ozone column (296.7 DU) of the twilight spectra and the negative of the y-intercept (*RCD*) represents the ozone *SCD* in the reference spectrum. An alternative method of deriving ozone *VCD*s is simply to divide slant column amounts by the *AMF* appropriate for the SZA (e.g., Sarkissan et al., 1997). Average slant column amounts for a set of twilight observations can then be calculated if ozone fields vary significantly during the observational period. In this work, ozone column densities were calculated using both methods, and the *VCD*s were found to be in close agreement (less than 2 DU difference).

Roscoe et al. (1994) observed that the Langley y-intercept contained an offset due to analytical artefacts, which was sensitive to changes in analytical parameters such as detector temperature and wavelength calibration. However, the Langley y-intercepts that we derived (see Fig. 4) were relatively consistent over the measurement period (12 twilight measurement sets). The mean intercept value was –583 DU and the standard deviation was ±18 DU. A slant column of 583 DU in the reference spectrum corresponds to a reference vertical column density of 364 DU by comparison with the calculated *AMF* (1.60). This indirect measurement of the noon reference ozone column density is high compared with the Brewer direct-sun ozone measurements on J-day 237, for which the value nearest in time to midday was 314 DU. A similar difference between the reference vertical column densities derived from Langley plots and from a Dobson spectrometer was reported by Roscoe et al. (1994).

The MANTRA campaign provided an excellent opportunity to compare ozone measurements made with the new ground-based spectrometer with measurements made using more established instruments (see Fig. 5); a brief description of the other instruments follows. Firstly, direct-sun measurements made using a Brewer spectrophotometer were obtained (Savastiouk and McElroy, this issue). Brewers are routinely used to make ozone column measurements (e.g., Kerr et al., 1988) with more than 150 instruments in operation worldwide. Ozone measurements are typically accurate to 1%, neglecting inaccuracies with the ozone-weighted temperature profile, which can induce a discrepancy as large as 2%. Measurement precision of the Brewer spectrophotometer is of the order of 1 DU. Secondly, ozonesondes, which employ an in situ chemical technique (Kohmyr, 1969) were launched routinely during the MANTRA campaign to provide vertical ozone profiles (Davies et al., 2000) that were integrated to derive total column measurements, shown in Fig. 5. Note that in this and all other figures, dates and times are in GMT.

Information from two different satellite instruments was also obtained. Total ozone measurements from the Earth Probe Total Ozone Mapping Spectrometer (TOMS) (Version 7) were downloaded from the TOMS Internet site (http://jwocky.gsfc.nasa.gov/) for Vanscoy (52° 01′N, 107° 02′W) and four other locations 1° away from the site (N, E, S, W). Consequently, a range of values was derived (the maximum and minimum values are given in Fig. 5). Figure 5 also includes measurements acquired from the Global Ozone Monitoring Experiment (GOME) satellite instrument (Level 2, Version 02.40) in the region around Vanscoy. For an overview of the GOME instrument, see Burrows et al. (1999b). Both sets of satellite observations indicated a degree of spatial variability in total ozone around the MANTRA measurement site, with the GOME measurements being slightly lower, consistent with a recent comparison between GOME, TOMS and TIROS Operational Vertical Sounder (TOVS) (Corlett et al., 2001). It should be noted that the grid of TOMS measurements was obtained by interpolating between individual point measurements, whereas the GOME measurements are simply the nearest point observations to the MANTRA site. It is likely that this is the major reason for the apparent differences in the spread of values between the two sets of satellite measurements.

The ozone measurements presented in Fig. 5 were made using distinctly different techniques. Inter-instrument agreement between the Brewer (direct sun viewing), ozonesondes (in situ chemical) and the zenith-sky viewing spectrometer was satisfactory (<5%) and consistent with the estimated error, and a useful validation of measurements made with the new instrument. There was broad agreement with the satellite measurements (<10%). Clearly, a more rigorous validation exercise involving comparison with other ground-based zenith-sky-viewing instruments over an extended period would be fruitful.

b *NO_2 Measurements*

While Langley plots present an elegant method for deriving ozone column information, they are less well suited to NO_2 due to the diurnal changes in the chemical partitioning between NO_2 and N_2O_5. The NO_2 vertical column increases throughout the day as N_2O_5 (a night-time reservoir species of NO_2) is photolyzed to produce NO_2. As part of our ongoing work to retrieve vertical profiles of NO_2 using the method described by Preston et al. (1997, 1998), it is necessary to employ a model that simulates NO_x partitioning (see Section 5 for further details). Such a model could also be used to create chemically modified Langley plots for NO_2 (Lee et al., 1994).

In the current work, each set of twilight NO_2 slant columns was plotted against increasing SZA (see Fig. 6 for a representative chart), and the *SCD* at 90° was interpolated from a smooth curve (fifth order polynomial) fitted to the data. Vertical column densities at 90° were calculated using Eq. (2). As noted above, Langley plots cannot be used to derive a value for the NO_2 *RCD* so the apparent NO_2 *RCD* was estimated from the twilight observations acquired on the same day as the reference spectrum by examining the increase in NO_2 *VCD* with SZA at high SZA. A best estimate of 7.8×10^{15} molecules cm^{-2} was obtained, and this amount was also

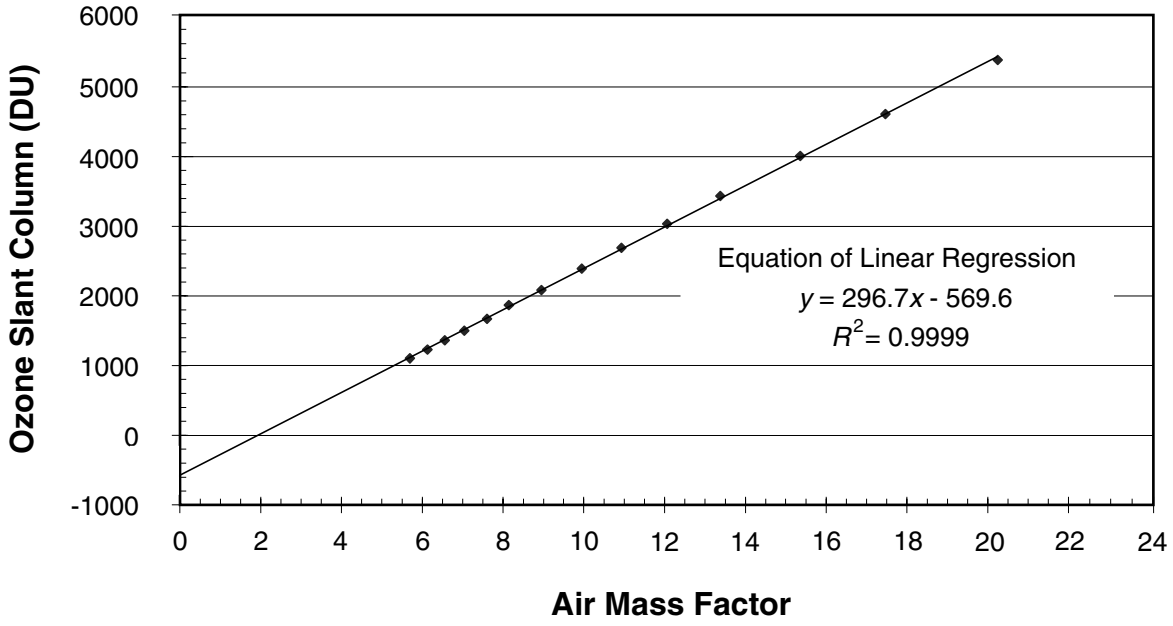

Fig. 3 Langley plot for ozone during sunset on Julian day 232 (20 August) 1998. The slope of the line indicates the vertical ozone column at twilight, and the negative of the y-intercept gives the slant column amount in the reference spectrum.

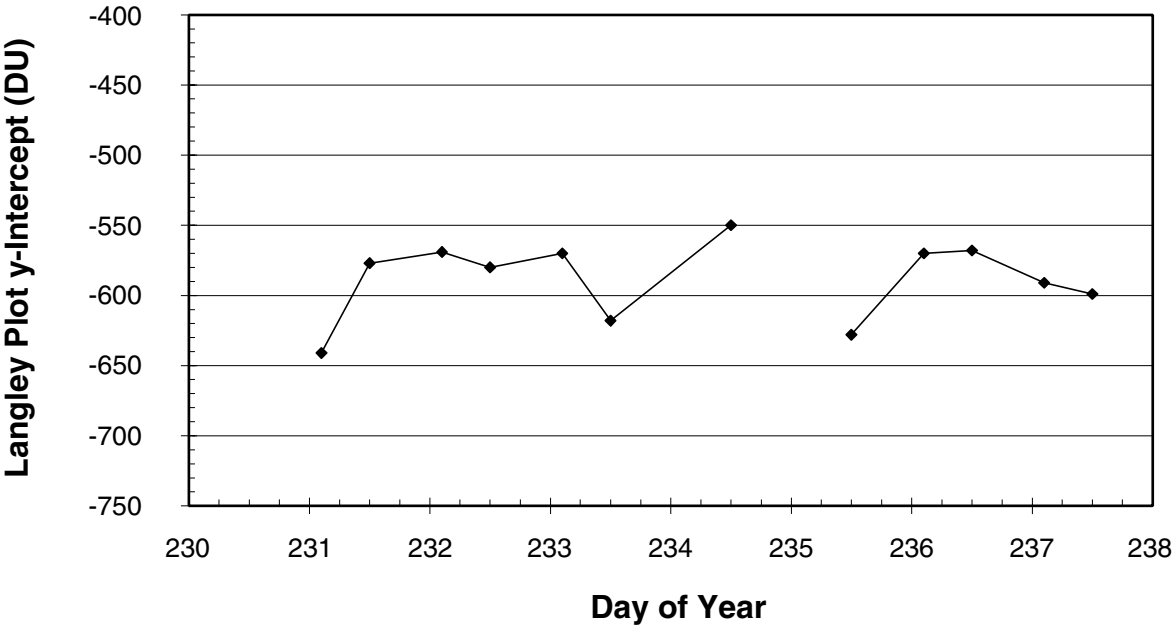

Fig. 4 Time series (GMT) of Langley-plot y-intercepts derived for ozone measurements during MANTRA 1998.

varied by up to $\pm 2 \times 10^{15}$ molecules cm^{-2} to quantify the error introduced in the NO_2 *VCD* by uncertainty in the *RCD* (as described in Section 3b).

Vertical column densities of NO_2 obtained during the MANTRA 1998 campaign are plotted in Fig. 7 and it can be seen that there was significant day-to-day variation in the retrieved NO_2 columns. It is possible that this variation is due solely to random errors in the measurements, although much of the error in the measurement is systematic and would be present as a constant offset to the true value. Therefore, while acknowledging the errors described in Section 3b and the limited dataset, there is some value in discussing the observations. The range of values for sunrise and sunset measurements was $3.0–3.5 \times 10^{15}$ molecules cm^{-2} and $4.2–4.6 \times 10^{15}$ molecules cm^{-2}, respectively. The cause of this variability is unlikely to be advection of polluted tropospheric air masses

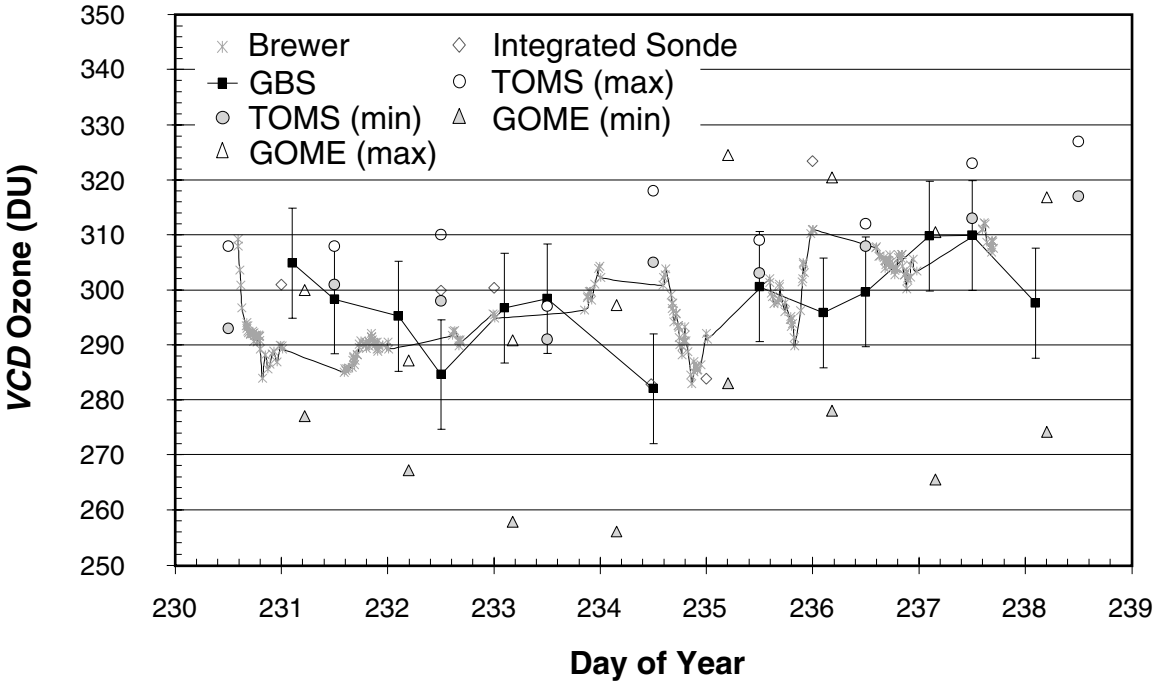

Fig. 5 Time series (GMT) of ozone vertical column densities measured by a suite of instruments during MANTRA 1998. GBS is the ground-based spectrometer used in this work.

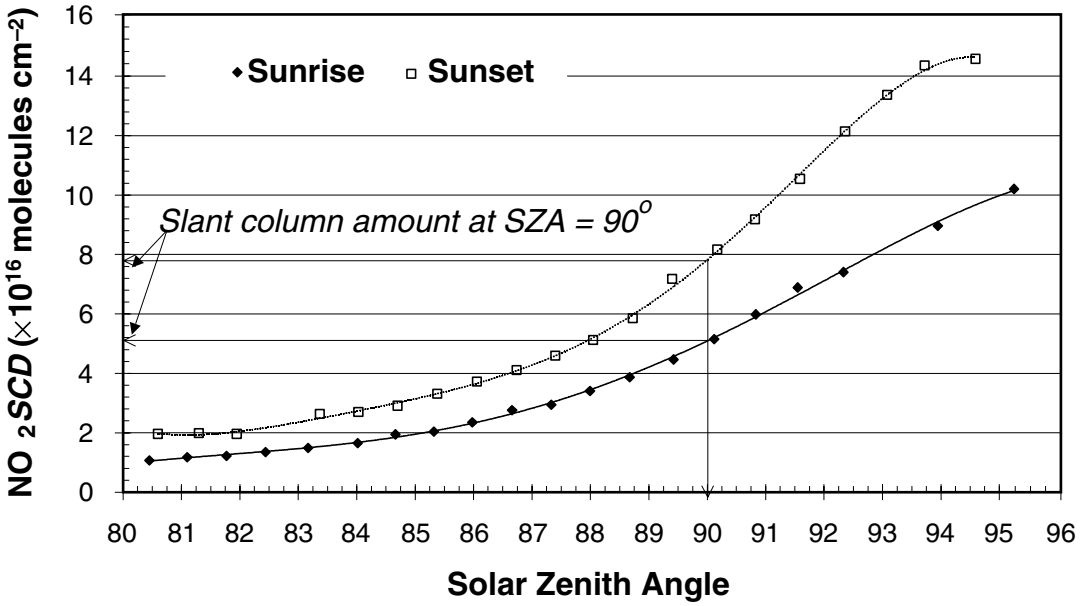

Fig. 6 NO_2 slant column densities measured during sunrise and sunset on Julian day 232 (20 August) 1998. The slant column at SZA = 90° is interpolated from the line of best fit to the data.

containing high NO_2 concentrations to the measurement site because Vanscoy is located at a distance from heavily populated areas. Previous studies (e.g., Roscoe et al., 1999) have shown that tropospheric pollution can adversely affect zenith-sky NO_2 at locations adjacent to urbanized regions.

The ground-based sunset measurements were compared with GOME observations (Level 2, Version 02.40). Overall, the day-to-day variation in the GOME NO_2 vertical columns followed a similar pattern to the ground-based measurements. However, there was some difference in the absolute values derived, with the GOME satellite measurements being consistently lower than those made using our instrument. This may be at least partly due to the 10:00 AM orbit of GOME, as the minimum NO_2 concentration occurs at 80–85° SZA, not

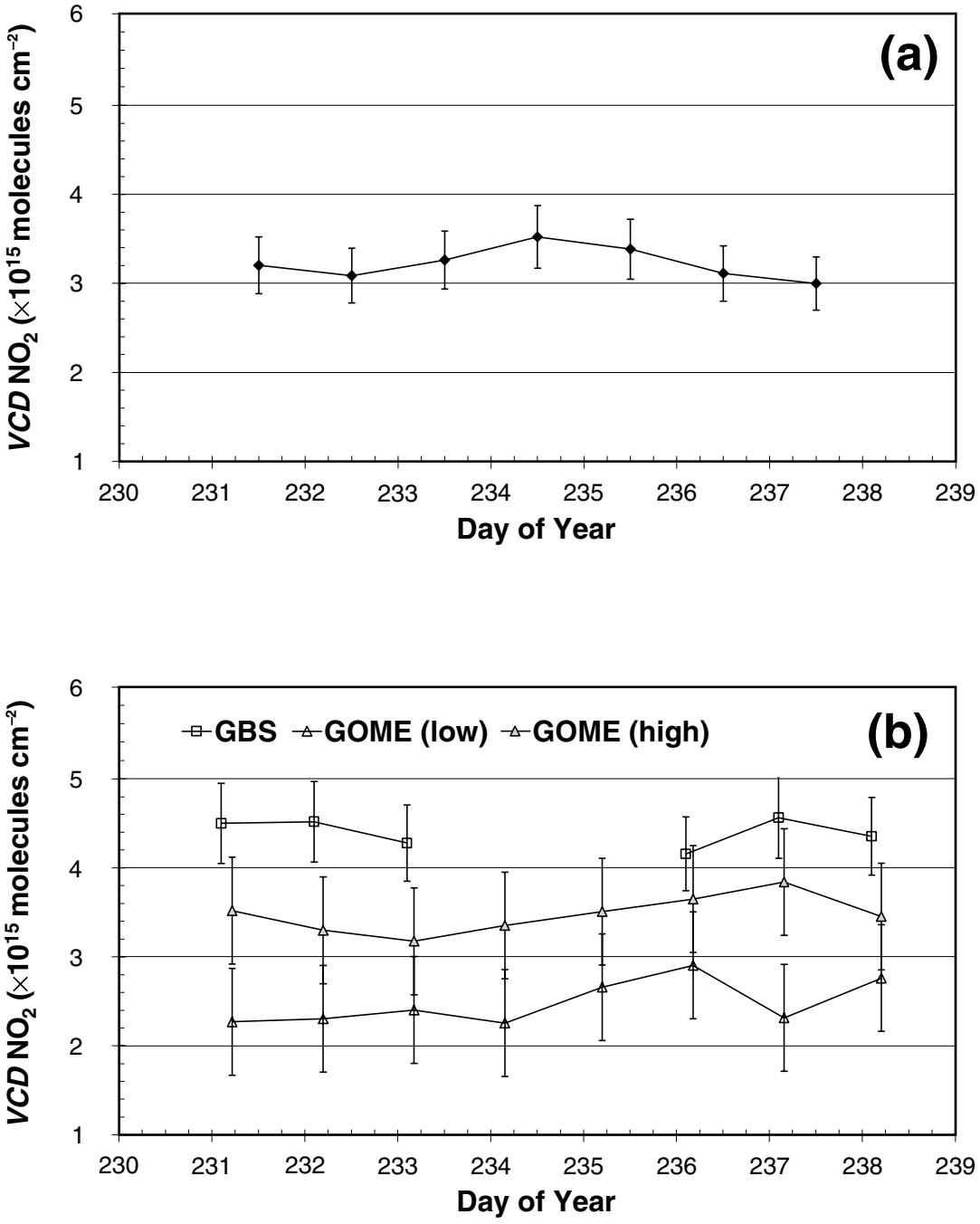

Fig. 7 Time series (GMT) of NO_2 vertical column densities measured by the ground-based spectrometer during MANTRA 1998 for (a) sunrise, and (b) sunset. The latter also includes maximum and minimum measurements from the GOME satellite instrument observed over a $5° \times 5°$ box around Vanscoy at sunset.

at 90° (sunrise) when the ground-based measurements were made. There was also often a substantial difference between the highest GOME NO_2 column observed in the Vanscoy region (within ±5° latitude or longitude) and the lowest column observed by GOME.

Representative measurements for the observation period were also obtained from the SAGE II satellite instrument. Typical NO_2 vertical column amounts measured by SAGE were of the order of 3.4×10^{15} molecules cm^{-2} for sunrise measurements and 6.2×10^{15} molecules cm^{-2} for sunset occultations. The SAGE sunrise measurements are in good agreement with the ground-based observations, however, the SAGE sunset measurements are approximately 25% higher than our observations, which in turn were approximately 25% higher than GOME observations. It would be interesting to carry out further intercomparisons with these and other instruments in an attempt to discern the cause of the apparent discrepancies. However, the photosensitive nature of NO_2 means that for a true comparison,

simultaneous measurements must be made with the same viewing geometry.

The average ratio of sunrise/sunset vertical columns measured using the ground-based spectrometer was calculated to be 0.72, with a standard deviation of 0.06. This value is compatible with the ratios of 0.6 and 0.7 reported by Koike et al. (1999) from summertime measurements made at two Japanese sites with latitudes similar to Vanscoy (43.4°N and 44.4°N). It is also in reasonable agreement with the results of McKenzie et al. (1991) measured at 45°S and adjusted for season, for which a ratio of 0.66 is derived using data in their Fig. 13 (based on NO_2 columns of approximately 3.8×10^{15} molecules cm^{-2} at sunrise and approximately 5.8×10^{15} molecules cm^{-2} at sunset). A box model having a comprehensive chemical scheme and accurate photolysis rates (Chartrand and McConnell, 1998) predicts a sunrise/sunset ratio of 0.60 for the NO_2 vertical columns given initial conditions appropriate for the MANTRA 1998 campaign, a value that is comparable with the measured ratio.

5 Conclusions and future work

A ground-based zenith-sky-viewing spectrometer has been constructed to make UV–visible measurements. It was developed to monitor stratospheric composition and has been demonstrated to operate successfully in a stand-alone manner. Total ozone columns recorded during the MANTRA 1998 field campaign compared favourably with established instruments, although a cross-comparison with other ground-based zenith-sky spectrometers is a necessary exercise to evaluate the system. Vertical NO_2 column densities were also measured during the MANTRA campaign and were in broad agreement with GOME measurements, although there appeared to be significant spatial and temporal variation in both sets of observations.

We are now pursuing several methods for the retrieval of profile information from the measured NO_2 slant columns. An optimal estimation approach based on that described by Preston et al. (1997, 1998) has been applied to the data, and will be compared to the co-located and simultaneous NO_2 profile measured with the UV-visible photodiode array spectrometer (McElroy, 1995) that was flown on the MANTRA balloon payload (Melo et al., this issue).

The instrument was also deployed at Environment Canada's Arctic Stratospheric Observatory at Eureka, NU (80.1°N, 86.4°W) in spring 1999, 2000 and 2001, and at Resolute Bay, NU (74.7°N, 94.6°W) in spring 2002. The resulting data are currently being analysed. Furthermore, improvements to the ground-based spectrometer system are continuing in our laboratory. One major avenue of ongoing work is the optical coupling of a star-tracking telescope to the spectrometer to facilitate night-time measurements of the target species, including NO_3. This would also allow measurements to be made during the polar night.

6 Acknowledgements

MRB was supported by funding from the Canadian Space Agency (CSA) and the Natural Sciences and Engineering Research Council of Canada (NSERC). The instrumentation was funded by NSERC and the field campaign was supported by CSA, the Meteorological Service of Canada, and the Centre for Research in Earth and Space Technology (CRESTech). The authors thank R. Dundas, J. Fromstein, E. Forsberg, K. Menzies, N. Jha, C. Heald and J. Halpine for assistance in developing the instrumentation and software, and D. Chartrand for the box model results discussed in Section 4b. We acknowledge the TOMS Ozone Processing Team of the National Aeronautics and Space Administration (NASA) Goddard Space Flight Center for making TOMS ozone measurements available on the internet, C. Zehner of the European Space Research Institute at the European Space Agency (ESRIN ESA) for his assistance in providing us with GOME satellite data, and S. Kim for her work in retrieving the relevant information for comparison.

The authors are grateful for the comments and suggestions made by three anonymous reviewers, which helped to improve the manuscript.

References

AUSTIN, J. and N. BUTCHART. 1994. The influence of climate change and the timing of stratospheric warmings on Arctic ozone depletion. *J. Geophys. Res.* **99**: 1127–1145.

BASSFORD, M.R.; K. STRONG and C.A. MCLINDEN. 2001. Zenith-sky observations of stratospheric gases: The sensitivity of air mass factors to geophysical parameters and the influence of tropospheric clouds. *J. Quant. Spectrosc. Radiat. Transfer,* **68**: 657–677.

BREWER, A.W.; C.T. MCELROY and J.B. KERR. 1973. Nitrogen dioxide concentrations in the atmosphere. *Nature*, **246**: 129–133.

BURROWS, J.P.; A. DEHN, B. DETERS, S. HIMMELMANN, A. RICHTER, S. VOIGT and J. ORPHAL. 1998. Atmospheric remote-sensing reference data from GOME: Part 1. Temperature dependent absorption cross-sections of NO_2 in the 231–794 nm range. *J. Quant. Spectrosc. Radiat. Transfer,* **60**: 1025–1031.

———; A. RICHTER, A. DEHN, B. DETERS, S. HIMMELMANN, S. VOIGT and J. ORPHAL. 1999a. Atmospheric remote-sensing reference data from GOME—2. Temperature dependent absorption cross-sections of O_3 in the 231–794 nm range. *J. Quant. Spectrosc. Radiat. Transfer,* **61**: 509–517.

———; M. WEBER, M. BUCHWITZ, V. ROZANOV, A. LADSTATTER-WEISSENMAYER, A. RICHTER, R. DEBEEK, R. HOOGEN, K. BRAMSTEDT, K.U. EICHMANN and M. EISINGER. 1999b. The global ozone monitoring experiment (GOME): Mission concept and first scientific results. *J. Atmos. Sci.* **56**: 127–150.

CHANCE, K.V. and R.J.D. SPURR. 1997. Ring effect studies: Rayleigh scattering, including molecular parameters for rotational Raman scattering, and the Fraunhofer spectrum. *Appl. Opt.* **36**: 5224–5230.

CHARTRAND, D.J. and J.C. MCCONNELL. 1998. Evidence of HBr production due to minor channel branching at mid-latitudes. *Geophys. Res. Lett.* **25**: 55–58.

CORLETT, G.K. and P.S. MONKS. 2001. A comparison of total column ozone values derived from the Global Ozone Monitoring Experiment (GOME), the Tiros Operational Vertical Sounder (TOVS), and the Total Ozone Mapping Spectrometer (TOMS). *J. Atmos. Sci.* **58**: 1103–1116.

DAVIES, J.; D.W. TARASICK, C.T. MCELROY, J.B. KERR, P.F. FOGAL and V. SAVASTIOUK. 2000. Evaluation of ECC ozonesonde preparation methods from laboratory tests and field comparisons during MANTRA. *In:* Proceedings of the Quadrennial Ozone Symposium, R.D. Bojkov and S. Kazuo (Eds), Hokkaido University, Sapporo, Japan, 3–8 July 2000, pp. 137–138.

DOBSON, G.M.B. 1957. Observer's handbook for the ozone spectrophotometer. *Ann. Int. Geophys. Year*, **5**: 46–89.

——— and D.N. HARRISON. 1926. Measurements of the amount of ozone in the Earth's atmosphere and its relation to other geophysical conditions. *Proc. R. Soc. A*, **110**: 660–693.

EISINGER, M.; A. RICHTER, A. LADSTATTER-WEIßENMAYER and J.P. BURROWS 1997. DOAS zenith sky observations: 1. BrO measurements over Bremen (53°) 1993–1994. *J. Atmos. Chem.* **26**: 93–108.

ERLE, F.; K. PFEILSTICKER and U. PLATT. 1995. On the influence of tropospheric clouds on zenith-scattered-light measurements of stratospheric species. *Geophys. Res. Lett.* **22:** 2725–2728.

FARMAN, J.C.; B.G. GARDINER and J.D. SHANKLIN. 1985. Large losses of total ozone in Antarctica reveal seasonal ClOx/NOx interaction. *Nature*, **315**: 207–210.

FIOLETOV, V.E.; J.B. KERR, D.I. WARDLE, J. DAVIES, E.W. HARE, C.T. MCELROY and D.W. TARASICK 1997. Long-term ozone decline over the Canadian Arctic to early 1997 from ground-based and balloon observations. *Geophys. Res. Lett.* **24**: 2705–2708.

FISH, D.J. and R.L. JONES. 1995. Rotational Raman scattering and the Ring effect in zenith-sky spectra. *Geophys. Res. Lett.* **22**: 811–814.

———; ——— and E.K. STRONG. 1995. Midlatitude observations of the diurnal variation of stratospheric BrO. *J. Geophys. Res.* **100**: 18863–18871.

GIL, M.; O. PUENTEDURA, M. YELA and E. CUEVAS. 2000. Behavior of NO_2 and O_3 columns during the eclipse of February 26, 1998, as measured by visible spectroscopy. *J. Geophys. Res.* **105**: 3583–3593.

GOUTAIL, F.; J.P. POMMEREAU, A. SARKISSIAN, E. KYRO and V. DOROKHOV. 1994. Total nitrogen dioxide at the Arctic polar circle since 1990. *Geophys. Res. Lett.* **21**: 1371–1374.

GREENBLATT, G.F.; J.J. ORLANDO, J.B. BURKHOLDER and A.R. RAVISHANKARA. 1990. Absorption measurements of oxygen between 330 and 1140 nm. *J. Geophys. Res.* **95**: 18577–18582.

HADJINICOLAOU, P.; J.P. PYLE, M.P. CHIPPERFIELD and J.A. KETTLEBOROUGH. 1997. Effect of interannual meteorological variability on mid-latitude O_3. *Geophys. Res. Lett.* **24**: 2993–2996.

HOFMANN, D.; P. BONASONI, M. DE MAZIERE, F. EVANGELISTI, G. GIOVANELLI, A. GOLDMAN, F. GOUTAIL, J. HARDER, R. JAKOUBEK, P. JOHNSTON, J. KERR, T. MCELROY, R. MCKENZIE, G. MOUNT, J.P. POMMEREAU, P. SIMON, S. SOLOMON, J. STUTZ, A. THOMAS, M. VAN ROOZENDAEL and E. WU. 1995. Intercomparison of UV/visible spectrometers for measurements of stratospheric NO_2 for the Network for the Detection of Stratospheric Change. *J. Geophys. Res.* **100**: 16765–16791.

KERR, J.B.; I.A. ASHBRIDGE and W.F.J. EVANS. 1998. Intercomparison of total ozone measured by the Brewer and Dobson spectrophotometers at Toronto. *J. Geophys. Res.* **93**: 11129–11140.

KOHMYR, W.D. 1969. Electrochemical concentration cells for gas analysis. *Ann. Geophys.* **25**: 203–210.

KOIKE, M.; Y. KONDO, W.A. MATTHEWS, P.V. JOHNSTON, H. NAKAJIMA, A. KAWAGUCHI, H. NAKANE, I. MURATA, A. BUDIYONO, M. KANADA and N. TORIYAMA. 1999. Assessment of the uncertainties in the NO_2 and O_3 measurements by visible spectrometers. *J. Atmos. Chem.* **32**: 121–145.

LEE, A.M.; H.K. ROSCOE, D.J. OLDHAM, J.A.C. SQUIRES, A. SARKISSIAN J.P. POMMEREAU and B.G. GARDINER. 1994. Improvements to the accuracy of measurements of NO_2 by zenith-sky visible spectrometers. *J. Quant. Spectrosc. Radiat. Transfer,* **52**: 649–657.

LILEY, J.B.; P.V. JOHNSTON, R.L. MCKENZIE, A.J. THOMAS and I.S. BOYD. 2000. Stratospheric NO_2 variations from a long time series at Lauder, New Zealand. *J. Geophys. Res.* **105**: 11633–11640.

MCELROY, C.T. 1995. A spectroradiometer for the measurement of direct and scattered solar spectral irradiance from on-board the NASA ER-2 high-altitude research aircraft. *Geophys. Res. Lett.* **22**: 1361–1364.

MCKENZIE, R.L.; P.V. JOHNSTON, C.T. MCELROY, J.B. KERR and S. SOLOMON. 1991. Altitude distributions of stratospheric constituents from ground-based measurements at twilight. *J. Geophys. Res.* **96**: 15499–15511.

MCLINDEN, C.A.; J.C. MCCONNELL, E. GRIFFIOEN and C.T. MCELROY. 2002. A vector radiative transfer model for the Odin/OSIRIS project. *Can. J. Phys.* **80**: 375–393.

MELO, S.M.L.; K. STRONG. M.R. BASSFORD, K.E. PRESTON, C.T. MCELROY, E.V. ROZANOV AND T. EGOROVA. 2005. Retrieval of stratospheric NO_2 vertical profiles from ground-based zenith-sky DOAS measurements: Results for the MANTRA 1998 field campaign. ATMOSPHERE-OCEAN, **43**: 339–350.

MOUNT, G.H.; R.W. SANDERS and J.W. BRAULT. 1992. Interference effects in reticon photodiode array detectors. *Appl. Optics,* **100**: 851–858.

NOXON, J.F. 1975. Nitrogen dioxide in the stratosphere and troposphere measured by ground-based absorption spectroscopy. *Science,* **187**: 547–549.

———; R.T. NORTON and W.R. HENDERSON. 1978. Observations of Atmospheric NO_3. *Geophys. Res. Lett*. **5**: 675–678.

———; E.C. WHIPPLE, JR. and R.S. HYDE. 1979. Stratospheric NO_2. 1. Observational method and behaviour at mid-latitude. *J. Geophys. Res.* **84**: 5047–5065.

OTTEN, C.; F. FERLEMANN, U. PLATT, T. WAGNER and K. PFEILSTICKER. 1998. Groundbased DOAS UV/visible measurements at Kiruna (Sweden) during the SESAME winters 1993/94 and 1994/95. *J. Atmos. Chem.* **30**: 141–162.

PERRIN, F.H. 1948. Whose absorption law? *J. Opt. Soc. Am.* **38**: 72–84.

PFEILSTICKER, K.; D.W. ARLANDER, J.P. BURROWS, F. ERLE, M. GIL, F. GOUTAIL, C. HERMANS, J.-C. LAMBERT, U. PLATT, J.-P. POMMEREAU, A. RICHTER, A. SARKISSIAN, M. VAN ROOZENDAEL, T. WAGNER and T. WINTERRATH. 1999a. Intercomparison of the influence of tropospheric clouds on UV-visible absorptions detected during the NDSC intercomparison campaign at OHP in June 1996. *Geophys. Res. Lett.* **26**: 1169–1172.

———; F. ERLE and U. PLATT. 1999b. Observation of the stratospheric NO_2 latitudinal distribution in the northern winter hemisphere. *J. Atmos. Chem.*, **32**: 101–120.

PLATT, U. 1994. Differential optical absorption spectroscopy (DOAS). In: *Air Monitoring by Spectroscopic Techniques*. M.W. Sigrist (Ed.), Chemical Analysis Series, Vol. 127, John Wiley and Sons, Inc., New York. 531 pp.

———; D. PERNER and H.W. PAETZ. 1979. Simultaneous measurement of atmospheric CH_2O, O_3 and NO_2 by differential optical absorption. *J. Geophys. Res.* **84**: 6329.

———; L. MARQUARD, T. WAGNER and D. PERNER. 1997. Corrections for zenith scattered light DOAS. *Geophys. Res. Lett.* **24**: 1759–1762.

POMMEREAU, J.P. and F. GOUTAIL. 1988. O_3 and NO_2 ground-based measurements by visible spectrometry during Arctic winter and spring 1988. *Geophys. Res. Lett.* **15**: 891–894.

PRESS, W.H.; B.P. FLANNERY, S.A. TEULOSKY and W.T. VETTERLING. 1992. *Numerical Recipes: The Art of Scientific Computing*. Cambridge University Press, Cambridge. 963 pp.

PRESTON, K.E.; R.L. JONES and H.K. ROSCOE. 1997. Retrieval of NO_2 vertical profiles from ground-based UV-visible measurements: Method and validation. *J. Geophys. Res.* **102**: 19089–19097.

———; D.J. FISH, H.K. ROSCOE and R.L. JONES. 1998. Accurate derivation of total and stratospheric vertical columns of NO_2 from ground-based zenith-sky measurements. *J. Atmos. Chem.* **30**: 163–172.

ROSCOE, H.K.; A.C. SQUIRES, D.J. OLDHAM, A. SARKISSIAN, J.-P. POMMEREAU and F. GOUTAIL. 1994. Improvements to the accuracy of zenith-sky measurements of total ozone by visible spectrometers. *J. Quant. Spectrosc. Radiat. Transfer,* **52**: 639–648.

———; D.J. FISH and R.L. JONES. 1996. Interpolation errors in UV-visible spectroscopy for stratospheric sensing: implications for sensitivity, spectral resolution, and spectral range. *Appl. Opt.* **35**: 427–432.

———; W.H. TAYLOR, J.D. EVANS, A.M. TAIT, R. FRESHWATER, D. FISH, E.K. STRONG and R.L. JONES. 1997. Automated ground-based star-pointing UV-visible spectrometer for stratospheric measurements. *Appl. Opt.* **36**: 6069–6075.

———; J.P. POMMEREAU, E. D'ALMEIDA, J. HOTTIER, C. COUREUL, R. DIDIER, I. PUNDT, L.M. BARTLETT, C.T. MCELROY, J.E. KERR, A. ELOKHOV, G. GIOVANELLI, F. RAVEGNANI, M. PREMUDA, I. KOSTADINOV, F. ERLE, T. WAGNER, K. PFEILSTICKER, M. KENNTNER, L.C. MARQUARD, M. GIL, O. PUENTEDURA, M. YELA, D.W. ARLANDER, B.A.K. HOISKAR, C.W. TELLEFSEN, K.K. TORNKVIST, B. HEESE, R.L. JONES, S.R. ALIWELL and R.A. FRESHWATER. 1999. Slant column measurements of O_3 and NO_2 during the NDSC intercomparison of zenith-sky UB-visible spectrometers in June 1996. *J. Atmos. Chem.* **32**: 281–314.

SARKISSIAN, A. 1992. Observation depuis le sol des nuages et des poussières dans l'atmosphère: applications à la stratosphère polaire et à l'atmosphère de Mars. Ph.D Thesis. Université de Paris 6.

———; G. VAUGHAN, H.K. ROSCOE, L.M. BARTLETT, F.M. O'CONNOR, D.G. DREW, P.A. HUGHES and D.M. MOORE. 1997. Accuracy of measurements of total ozone by a SAOZ ground-based zenith sky visible spectrometer. *J. Geophys. Res*. **102**: 1379–1390.

SAVASTIOUK, S. and C.T. MCELROY. 2005. Brewer spectrophotometer total ozone measurements made during the 1998 Middle Atmosphere Nitrogen Trend Assessment (MANTRA) campaign. ATMOSPHERE-OCEAN, **43**: 315–324.

SHINDELL. D.T.; D. RIND and P. LONERGAN. 1998. Increased polar stratospheric ozone losses and delayed eventual recovery owing to increasing greenhouse-gas concentrations. *Nature,* **392**: 588–592.

SIORIS C.E. and W.F.J. EVANS. 1999. Filling in of Fraunhofer and gas-absorption lines in sky spectra as caused by rotational Raman scattering. *Appl. Opt.* **38**: 2706–2713.

SOLOMON, S.; G.H MOUNT, R.W. SANDERS and A.L. SCHMELTEKOPF. 1987a. Visible spectroscopy at McMurdo station, Antarctica, 2, Observations of OClO. *J. Geophys. Res.* **92**: 8329–8338.

———; A.L. SCHMELTEKOPF and R.W. SANDERS. 1987b. On the interpretation of zenith sky absorption measurements. *J. Geophys. Res.* **92**: 8311–8319.

———; R.W. SANDERS, M.A. CARROLL and A.L. SCHMELTEKOPF. 1989. Visible and ultraviolet spectroscopy at McMurdo Station, Antarctica, 5, Observations of the diurnal variations of BrO and OClO. *J. Geophys. Res.,* **94**: 11393–11403.

STRONG, K.; G. BAILAK, BARTON, M.R. BASSFORD, R.D. BLATHERWICK, S. BROWN, D. CHARTRAND, J. DAVIES, J.R. DRUMMOND, P.F. FOGAL, E. FORSBERG, R. HALL, A. JOFRE, J. KAMINSKI, J. KOSTERS, C. LAURIN, J.C. MCCONNELL, C.T. MCELROY, C.A. MCLINDEN, S.M.L. MELO, K. MENZIES, C. MIDWINTER, F.J. MURCRAY, C. NOWLAN, R.J. OLSON, B.M. QUINE, Y. ROCHON, V. SAVASTIOUK, B. SOLHEIM, D. SOMMERFELDT, A. ULLBERG, S. WERCHOHLAD, H. WU and D. WUNCH. 2005. MANTRA – A balloon mission to study the odd-nitrogen budget of the stratosphere. ATMOSPHERE-OCEAN, **43**: 283–299.

STUTZ, J. and U. PLATT. 1992. Problems in using diode arrays for open path DOAS measurements of atmospheric species. SPIE Vol. 1715 Optical Methods in Atmospheric Chemistry, pp. 329–340.

SYED, M.Q. and A.W. HARRISON. 1980. Ground based observations of stratospheric nitrogen dioxide. *Can J. Phys.* **58**: 788–502.

THOMASON, L.W.; L.R. POOLE and T. DESHLER. 1997. A global climatology of stratospheric aerosol surface area density deduced from Stratospheric Aerosol and Gas Experiment II measurements: 1984–1994. *J. Geophys. Res.* **102**: 8967–8976.

VAN ROOZENDAEL, M.; M. DE MAZIERE and P.C. SIMON. 1994. Ground-based visible measurements at the Jungfraujoch Station since 1990. *J. Quant. Spectrosc. Radiat. Transfer,* **52**: 231–240.

VANDAELE, A.C.; C. HERMANS, P.C. SIMON, M. CARLEER, R. COLIN, S. FALLY, M.F. MERIENNE, A. JENOUVRIER and B. COQUART. 1998. Measurements of the NO_2 absorption cross-section from 42000 cm^{-1} to 10000 cm^{-1} (238–1000 nm) at 220 K and 294 K. *J. Quant. Spectrosc. Radiat. Transfer,* **59**: 171–184.

VAUGHAN, G.; H.K. ROSCOE, L.M. BARTLETT, F.M. O'CONNOR, A. SARKISSIAN, ; M. VAN ROOZENDAEL, J.C. LAMBERT, P.C. SIMON, K. KARLSEN, B.A.K. HOISKAR, D.J. FISH, R.L. JONES, R.A. FRESHWATER, J.P. POMMEREAU, F. GOUTAIL, S.B. ANDERSEN, D.G. DREW, P.A. HUGHES, D. MOORE, J. MELLQVIST, E. HEGELS, T. KLUPFEL, F. ERLE, K. PFEILSTICKER and U. PLATT. 1997. An intercomparison of ground-based UV-visible sensors of ozone and NO_2. *J. Geophys. Res.* **102**: 1411–1422.

WMO. 1999. Scientific assessment of ozone depletion: 1998. Report No. 44, Global Ozone Research and Monitoring Project: WMO, Geneva.